EUROPEAN ORGANISATION FOR NUCLEAR RESEARCH

CERN-PPE/96-098
18 July 1996

Test of the Four-Fermion Contact Interaction in e^+e^- Collisions at 130-140 GeV

The OPAL Collaboration

Abstract

The differential cross-sections for $e^+e^- \to e^+e^-$, $e^+e^- \to \mu^+\mu^-$ and $e^+e^- \to \tau^+\tau^-$, and the total cross-section for $e^+e^- \to q\bar{q}$ at centre-of-mass energies of 130-140 GeV were studied using about 5 pb^{-1} of data collected with the OPAL detector at LEP in October and November 1995. The results are in agreement with the Standard Model predictions. Four-fermion contact interaction models were fitted to the data and lower limits were obtained on the energy scale Λ at the 95 % confidence level.

(Submitted to Physics Letters B)

The OPAL Collaboration

G. Alexander[23], J. Allison[16], N. Altekamp[5], K. Ametewee[25], K.J. Anderson[9], S. Anderson[12], S. Arcelli[2], S. Asai[24], D. Axen[29], G. Azuelos[18,a], A.H. Ball[17], E. Barberio[8], R.J. Barlow[16], R. Bartoldus[3], J.R. Batley[5], J. Bechtluft[14], C. Beeston[16], T. Behnke[8], A.N. Bell[1], K.W. Bell[20], G. Bella[23], S. Bentvelsen[8], P. Berlich[10], S. Bethke[14], O. Biebel[14], V. Blobel[8], I.J. Bloodworth[1], J.E. Bloomer[1], M. Bobinski[10], P. Bock[11], H.M. Bosch[11], M. Boutemeur[34], B.T. Bouwens[12], S. Braibant[12], R.M. Brown[20], H.J. Burckhart[8], C. Burgard[8], R. Bürgin[10], P. Capiluppi[2], R.K. Carnegie[6], A.A. Carter[13], J.R. Carter[5], C.Y. Chang[17], C. Charlesworth[6], D.G. Charlton[1,b], D. Chrisman[4], S.L. Chu[4], P.E.L. Clarke[15], I. Cohen[23], J.E. Conboy[15], O.C. Cooke[16], M. Cuffiani[2], S. Dado[22], C. Dallapiccola[17], G.M. Dallavalle[2], S. De Jong[12], L.A. del Pozo[8], K. Desch[3], M.S. Dixit[7], E. do Couto e Silva[12], M. Doucet[18], E. Duchovni[26], G. Duckeck[34], I.P. Duerdoth[16], J.E.G. Edwards[16], P.G. Estabrooks[6], H.G. Evans[9], M. Evans[13], F. Fabbri[2], P. Fath[11], F. Fiedler[12], M. Fierro[2], H.M. Fischer[3], R. Folman[26], D.G. Fong[17], M. Foucher[17], A. Fürtjes[8], P. Gagnon[7], A. Gaidot[21], J.W. Gary[4], J. Gascon[18], S.M. Gascon-Shotkin[17], N.I. Geddes[20], C. Geich-Gimbel[3], F.X. Gentit[21], T. Geralis[20], G. Giacomelli[2], P. Giacomelli[4], R. Giacomelli[2], V. Gibson[5], W.R. Gibson[13], D.M. Gingrich[30,a], D. Glenzinski[9], J. Goldberg[22], M.J. Goodrick[5], W. Gorn[4], C. Grandi[2], E. Gross[26], M. Gruwé[8], C. Hajdu[32], G.G. Hanson[12], M. Hansroul[8], M. Hapke[13], C.K. Hargrove[7], P.A. Hart[9], C. Hartmann[3], M. Hauschild[8], C.M. Hawkes[5], R. Hawkings[8], R.J. Hemingway[6], G. Herten[10], R.D. Heuer[8], M.D. Hildreth[8], J.C. Hill[5], S.J. Hillier[1], T. Hilse[10], P.R. Hobson[25], R.J. Homer[1], A.K. Honma[28,a], D. Horváth[32,c], R. Howard[29], R.E. Hughes-Jones[16], D.E. Hutchcroft[5], P. Igo-Kemenes[11], D.C. Imrie[25], M.R. Ingram[16], K. Ishii[24], A. Jawahery[17], P.W. Jeffreys[20], H. Jeremie[18], M. Jimack[1], A. Joly[18], C.R. Jones[5], G. Jones[16], M. Jones[6], R.W.L. Jones[8], U. Jost[11], P. Jovanovic[1], T.R. Junk[8], D. Karlen[6], K. Kawagoe[24], T. Kawamoto[24], R.K. Keeler[28], R.G. Kellogg[17], B.W. Kennedy[20], B.J. King[8], J. Kirk[29], S. Kluth[8], T. Kobayashi[24], M. Kobel[10], D.S. Koetke[6], T.P. Kokott[3], S. Komamiya[24], R. Kowalewski[8], T. Kress[11], P. Krieger[6], J. von Krogh[11], P. Kyberd[13], G.D. Lafferty[16], H. Lafoux[21], R. Lahmann[17], W.P. Lai[19], D. Lanske[14], J. Lauber[15], S.R. Lautenschlager[31], J.G. Layter[4], D. Lazic[22], A.M. Lee[31], E. Lefebvre[18], D. Lellouch[26], J. Letts[2], L. Levinson[26], C. Lewis[15], S.L. Lloyd[13], F.K. Loebinger[16], G.D. Long[17], M.J. Losty[7], J. Ludwig[10], A. Luig[10], A. Malik[21], M. Mannelli[8], S. Marcellini[2], C. Markus[3], A.J. Martin[13], J.P. Martin[18], G. Martinez[17], T. Mashimo[24], W. Matthews[25], P. Mättig[3], W.J. McDonald[30], J. McKenna[29], E.A. Mckigney[15], T.J. McMahon[1], A.I. McNab[13], R.A. McPherson[8], F. Meijers[8], S. Menke[3], F.S. Merritt[9], H. Mes[7], J. Meyer[27], A. Michelini[2], G. Mikenberg[26], D.J. Miller[15], R. Mir[26], W. Mohr[10], A. Montanari[2], T. Mori[24], M. Morii[24], U. Müller[3], K. Nagai[26], I. Nakamura[24], H.A. Neal[8], B. Nellen[3], B. Nijjhar[16], R. Nisius[8], S.W. O'Neale[1], F.G. Oakham[7], F. Odorici[2], H.O. Ogren[12], T. Omori[24], M.J. Oreglia[9], S. Orito[24], J. Pálinkás[33,d], G. Pásztor[32], J.R. Pater[16], G.N. Patrick[20], J. Patt[10], M.J. Pearce[1], S. Petzold[27], P. Pfeifenschneider[14], J.E. Pilcher[9], J. Pinfold[30], D.E. Plane[8], P. Poffenberger[28], B. Poli[2], A. Posthaus[3], H. Przysiezniak[30], D.L. Rees[1], D. Rigby[1], S.A. Robins[13], N. Rodning[30], J.M. Roney[28], A. Rooke[15], E. Ros[8], A.M. Rossi[2], M. Rosvick[28], P. Routenburg[30], Y. Rozen[22], K. Runge[10], O. Runolfsson[8], U. Ruppel[14], D.R. Rust[12], R. Rylko[25], K. Sachs[10], E.K.G. Sarkisyan[23], M. Sasaki[24], C. Sbarra[2], A.D. Schaile[34], O. Schaile[34], F. Scharf[3], P. Scharff-Hansen[8], P. Schenk[4], B. Schmitt[8], S. Schmitt[11], M. Schröder[8], H.C. Schultz-Coulon[10], M. Schulz[8], M. Schumacher[3], P. Schütz[3], W.G. Scott[20], T.G. Shears[16], B.C. Shen[4], C.H. Shepherd-Themistocleous[27], P. Sherwood[15], G.P. Siroli[2], A. Sittler[27], A. Skillman[15], A. Skuja[17], A.M. Smith[8], T.J. Smith[28], G.A. Snow[17], R. Sobie[28], S. Söldner-Rembold[10], R.W. Springer[30], M. Sproston[20], A. Stahl[3],

M. Starks[12], M. Steiert[11], K. Stephens[16], J. Steuerer[27], B. Stockhausen[3], D. Strom[19], F. Strumia[8], P. Szymanski[20], R. Tafirout[18], S.D. Talbot[1], S. Tanaka[24], P. Taras[18], S. Tarem[22], M. Tecchio[8], M. Thiergen[10], M.A. Thomson[8], E. von Törne[3], S. Towers[6], T. Tsukamoto[24], E. Tsur[23], A.S. Turcot[9], M.F. Turner-Watson[8], P. Utzat[11], R. Van Kooten[12], G. Vasseur[21], M. Verzocchi[10], P. Vikas[18], M. Vincter[28], E.H. Vokurka[16], F. Wäckerle[10], A. Wagner[27], C.P. Ward[5], D.R. Ward[5], J.J. Ward[15], P.M. Watkins[1], A.T. Watson[1], N.K. Watson[7], P. Weber[6], P.S. Wells[8], N. Wermes[3], J.S. White[28], B. Wilkens[10], G.W. Wilson[27], J.A. Wilson[1], G. Wolf[26], S. Wotton[5], T.R. Wyatt[16], S. Yamashita[24], G. Yekutieli[26], V. Zacek[18],

[1]School of Physics and Space Research, University of Birmingham, Birmingham B15 2TT, UK
[2]Dipartimento di Fisica dell' Università di Bologna and INFN, I-40126 Bologna, Italy
[3]Physikalisches Institut, Universität Bonn, D-53115 Bonn, Germany
[4]Department of Physics, University of California, Riverside CA 92521, USA
[5]Cavendish Laboratory, Cambridge CB3 0HE, UK
[6] Ottawa-Carleton Institute for Physics, Department of Physics, Carleton University, Ottawa, Ontario K1S 5B6, Canada
[7]Centre for Research in Particle Physics, Carleton University, Ottawa, Ontario K1S 5B6, Canada
[8]CERN, European Organisation for Particle Physics, CH-1211 Geneva 23, Switzerland
[9]Enrico Fermi Institute and Department of Physics, University of Chicago, Chicago IL 60637, USA
[10]Fakultät für Physik, Albert Ludwigs Universität, D-79104 Freiburg, Germany
[11]Physikalisches Institut, Universität Heidelberg, D-69120 Heidelberg, Germany
[12]Indiana University, Department of Physics, Swain Hall West 117, Bloomington IN 47405, USA
[13]Queen Mary and Westfield College, University of London, London E1 4NS, UK
[14]Technische Hochschule Aachen, III Physikalisches Institut, Sommerfeldstrasse 26-28, D-52056 Aachen, Germany
[15]University College London, London WC1E 6BT, UK
[16]Department of Physics, Schuster Laboratory, The University, Manchester M13 9PL, UK
[17]Department of Physics, University of Maryland, College Park, MD 20742, USA
[18]Laboratoire de Physique Nucléaire, Université de Montréal, Montréal, Quebec H3C 3J7, Canada
[19]University of Oregon, Department of Physics, Eugene OR 97403, USA
[20]Rutherford Appleton Laboratory, Chilton, Didcot, Oxfordshire OX11 0QX, UK
[21]CEA, DAPNIA/SPP, CE-Saclay, F-91191 Gif-sur-Yvette, France
[22]Department of Physics, Technion-Israel Institute of Technology, Haifa 32000, Israel
[23]Department of Physics and Astronomy, Tel Aviv University, Tel Aviv 69978, Israel
[24]International Centre for Elementary Particle Physics and Department of Physics, University of Tokyo, Tokyo 113, and Kobe University, Kobe 657, Japan
[25]Brunel University, Uxbridge, Middlesex UB8 3PH, UK
[26]Particle Physics Department, Weizmann Institute of Science, Rehovot 76100, Israel
[27]Universität Hamburg/DESY, II Institut für Experimental Physik, Notkestrasse 85, D-22607 Hamburg, Germany
[28]University of Victoria, Department of Physics, P O Box 3055, Victoria BC V8W 3P6, Canada
[29]University of British Columbia, Department of Physics, Vancouver BC V6T 1Z1, Canada

[30]University of Alberta, Department of Physics, Edmonton AB T6G 2J1, Canada
[31]Duke University, Dept of Physics, Durham, NC 27708-0305, USA
[32]Research Institute for Particle and Nuclear Physics, H-1525 Budapest, P O Box 49, Hungary
[33]Institute of Nuclear Research, H-4001 Debrecen, P O Box 51, Hungary
[34]Ludwigs-Maximilians-Universität München, Sektion Physik, Am Coulombwall 1, D-85748 Garching, Germany

[a] and at TRIUMF, Vancouver, Canada V6T 2A3
[b] and Royal Society University Research Fellow
[c] and Institute of Nuclear Research, Debrecen, Hungary
[d] and Department of Experimental Physics, Lajos Kossuth University, Debrecen, Hungary

1 Introduction

The measurements at LEP at 130-140 GeV have provided the first e^+e^- collision data at energies well above the Z^0 resonance. The cross-sections and angular distributions for $e^+e^- \to q\bar{q}$ and $e^+e^- \to \ell^+\ell^-$ ($\ell = e, \mu, \tau$) have been observed by OPAL to be in good agreement with Standard Model expectations [1]. It is interesting to see what constraints are set by these data on possible contributions from new physics.

Here we study the four-fermion contact interaction [2]. The basic idea is that the Standard Model is a part of a more general theory characterised by an energy scale Λ and the consequences of the theory are observed at energies well below Λ as a deviation from the Standard Model which can be described by an effective contact interaction. In the context of composite models of leptons and quarks, the contact interaction is regarded as a remnant of the binding force between the substructure of fermions. If electrons are composite such an effect would appear in Bhabha scattering ($e^+e^- \to e^+e^-$). If the other leptons and quarks share the same type of substructure, the contact interaction would exist also in the processes $e^+e^- \to \mu^+\mu^-, \tau^+\tau^-$ and $e^+e^- \to q\bar{q}$. More generally, the contact interaction is considered to be a convenient parametrisation to describe a possible deviation from the Standard Model, which may be caused by some new physics.

Analyses of such contact interactions have been performed at lower energy experiments for the processes $e^+e^- \to \ell^+\ell^-$ [3–10] and $e^+e^- \to q\bar{q}$ [5, 11]. It is expected that the sensitivity of the measurements to the contact interaction will increase with centre-of-mass energy ($\sqrt{s}$) due to the decrease of the Standard Model cross-section as $1/s$, while some contributions of the contact interaction stay constant or even increase in proportion to s [12]. Here we present a contact interaction analysis of the $e^+e^- \to e^+e^-$, $e^+e^- \to \mu^+\mu^-$, $e^+e^- \to \tau^+\tau^-$ and $e^+e^- \to q\bar{q}$ channels using OPAL data at centre-of-mass energies of 130-140 GeV. The cross-sections are compared with expectations of contact interaction models in order to set lower limits on the energy scale Λ.

2 Four-fermion contact interaction

In the contact interaction approach, the Standard Model contribution remains unchanged, but an effective new interaction is added to it. Following the notation in [13], the effective Lagrangian for the four-fermion contact interaction in the process $e^+e^- \to f\bar{f}$ is defined by :

$$\mathcal{L}^{\text{contact}} = \frac{g^2}{(1+\delta)\Lambda^2} \sum_{i,j=L,R} \eta_{ij} [\bar{e}_i \gamma^\mu e_i][\bar{f}_j \gamma_\mu f_j] \qquad (1)$$

with

$$\delta = \begin{cases} 1 & f = e \\ 0 & f \neq e \end{cases} .$$

Here e_L and e_R (f_L and f_R) are chirality projections of electron (fermion) spinors. The unknown coefficients η_{ij} determine the type of chiral coupling of the four fermions, L and R denote left- and right-handed currents, respectively, and Λ is the energy scale of the contact interaction.

By convention, the unknown coupling constant g is set to $g^2/4\pi = 1$ and $|\eta_{ij}| \leq 1$. For the process $e^+e^- \to e^+e^-$, the size of the contact interaction differs from the other channels by a statistical factor of 1/2. A number of different models (choice of η_{ij} parameters) are customarily considered. They are summarised in table 1. The VV and AA denote the vector and axial vector couplings, respectively. The signs ($\pm$) of the η_{ij} indicate positive or negative interference with the Standard Model amplitude.

In the presence of the contact interaction the differential cross-section for $e^+e^- \to f\bar{f}$, as a function of the polar angle θ of the outgoing fermion with respect to the e^- beam direction, can be written to lowest order as:

$$\begin{aligned}\frac{1}{F_C}\frac{4s}{\pi\alpha^2}\frac{d\sigma}{d\cos\theta} &= \left[|\tilde{A}^{ee}_{LR}(t)|^2 + |\tilde{A}^{ee}_{RL}(t)|^2\right]\left(\frac{s}{t}\right)^2\delta \\ &+ \left[|A^{ef}_{LR}(s)|^2 + |A^{ef}_{RL}(s)|^2\right]\left(\frac{t}{s}\right)^2 \\ &+ \left[|A^{ef}_{LL}(s)|^2 + |A^{ef}_{RR}(s)|^2\right]\left(\frac{u}{s}\right)^2 \qquad (2)\end{aligned}$$

with $t = -\frac{1}{2}s(1-\cos\theta)$ and $u = -\frac{1}{2}s(1+\cos\theta)$. The overall colour factor F_C is 1 for $\ell^+\ell^-$ and 3 for $q\bar{q}$. The helicity amplitudes are:

$$\tilde{A}^{ee}_{ij}(t) = Q_e^2 + g_i^e g_j^e \chi(t) + \eta_{ij}\frac{t}{\alpha}\frac{1}{\Lambda^2} \qquad (i \neq j) \qquad (3)$$

$$A^{ef}_{ij}(s) = Q_e Q_f + g_i^e g_j^f \chi(s) + \eta_{ij}\frac{s}{\alpha}\frac{1}{\Lambda^2} \qquad (i \neq j) \qquad (4)$$

$$A^{ef}_{ij}(s) = Q_e Q_f + g_i^e g_j^f [\chi(s) + \frac{s}{t}\chi(t)\delta] + \frac{s}{t}\delta + (1+\delta)\eta_{ij}\frac{s}{\alpha}\frac{1}{\Lambda^2} \qquad (i = j). \qquad (5)$$

Here α is the electromagnetic coupling constant. The left- and right-handed couplings, g_L^f and g_R^f, of the fermion f to the Z^0 are given by

$$g_L^f = \frac{e}{\sin\theta_W \cos\theta_W}(I_3 - Q_f \sin^2\theta_W) \ , \qquad g_R^f = \frac{e}{\sin\theta_W \cos\theta_W}(-Q_f \sin^2\theta_W) \ ,$$

where e is the electron charge, Q_f is the electric charge in units of $|e|$ of the fermion f, I_3 is the third component of the weak isospin and θ_W is the electroweak mixing angle. The s- and t-channel Z^0 propagators are

$$\chi(s) = s/(s - M_Z^2 + is\Gamma_Z/M_Z), \qquad \chi(t) = t/(t - M_Z^2).$$

It should be noted that the LR and RL models give identical results for lepton pair channels while for the $q\bar{q}$ final state the results of the LR and RL models are different.

The cross-section formula (2) can be decomposed into three parts

$$\frac{d\sigma}{d\cos\theta} = SM^0(s,t) + C_2^0(s,t)\frac{1}{\Lambda^2} + C_4^0(s,t)\frac{1}{\Lambda^4} \ . \qquad (6)$$

The first term denotes the Standard Model cross-section. The second and third terms come from the contact interaction and represent deviations from the Standard Model expectation. The C_2^0 term comes from the interference of the contact interaction with the Standard Model amplitude and the C_4^0 term from the square of the contact interaction amplitude. The coefficients $C_2^0(s,t)$ and $C_4^0(s,t)$ have different dependences on s and t depending on the final state fermion and the choice of the contact interaction model.

3 Data sample

A feature of e^+e^- collision data at centre-of-mass energies well above the Z^0 resonance is a tendency for radiative return to the Z^0 by emitting initial-state radiation photons which reduces the effective centre-of-mass energy, $\sqrt{s'}$, of the subsequent e^+e^- collision to the region of the Z^0 resonance. Here we consider the cross-sections for $e^+e^- \to e^+e^-$, $e^+e^- \to \mu^+\mu^-$, $e^+e^- \to \tau^+\tau^-$ and $e^+e^- \to q\bar{q}$ at large $\sqrt{s'}$ so excluding the events from radiative return to the Z^0. The selection of such an event sample and the luminosity measurement are described in [1]. For the $e^+e^- \to \mu^+\mu^-, \tau^+\tau^-$ and $e^+e^- \to q\bar{q}$ channels $s'/s > 0.8$ was required. An almost equivalent cut was applied to the $e^+e^- \to e^+e^-$ sample using a cut on the maximum acollinearity angle at 10°. The integrated luminosity of the data sample is about 5.2 pb^{-1} divided among three centre-of-mass energies of 130.26 GeV (2.7 pb^{-1}), 130.23 GeV (2.5 pb^{-1}) and 140 GeV (0.05 pb^{-1}). The numbers of events used in this analysis were 967 $e^+e^- \to e^+e^-$, 53 $e^+e^- \to \mu^+\mu^-$, 19 $e^+e^- \to \tau^+\tau^-$ and 334 $e^+e^- \to q\bar{q}$ events[1]. The systematic errors of the event selection are 2.4 % ($e^+e^- \to e^+e^-$), 2.0 % ($e^+e^- \to \mu^+\mu^-$), 2.8 % ($e^+e^- \to \tau^+\tau^-$) and 4.0 % ($e^+e^- \to q\bar{q}$). The luminosity error was estimated to be 1 %.

The angular distributions of the leptonic channels are expressed in 9 bins over $-0.9 < \cos\theta < 0.9$ for $e^+e^- \to e^+e^-$, and 10 bins over $-1.0 < \cos\theta < 1.0$ for the $e^+e^- \to \mu^+\mu^-$ and $\tau^+\tau^-$ channels. The results are summarised in table 2 together with the corresponding values of the differential cross-sections. For the $e^+e^- \to q\bar{q}$ channel only the total cross-sections given in [1] were used in this analysis.

4 Calculation of predicted cross-sections

In order to compare the model with the data, the lowest order cross-section (6) must be corrected for electroweak and QED radiative effects and the expected cross-section calculated taking into account the experimental cuts. The $e^+e^- \to q\bar{q}$ channel must be corrected also for QCD effects. Different approaches were used for the Standard Model part and for the contact interaction terms.

The Standard Model cross-sections were calculated for each $\cos\theta$ bin and centre-of-mass energy using ALIBABA [14] for $e^+e^- \to e^+e^-$, and ZFITTER [15] for $e^+e^- \to \mu^+\mu^-, \tau^+\tau^-$ and $q\bar{q}$ with the cut on the acollinearity angle (e^+e^-) or s' ($\mu^+\mu^-$, $\tau^+\tau^-$ and $q\bar{q}$) at the same value as in the data sample. The systematic uncertainty of these predictions is estimated to be 2.5 %, 1.0 % and 2.0 % for the $e^+e^- \to e^+e^-$, $e^+e^- \to \mu^+\mu^-/\tau^+\tau^-$ and $e^+e^- \to q\bar{q}$ channels, respectively.[2] The Standard Model parameters were fixed at $M_Z = 91.188$ GeV, $M_{top} = 180$ GeV and $M_{Higgs} = 100$ GeV. The dependences of the cross-section on these parameters within their uncertainties are negligible compared to the sensitivity of the present fit.

[1] The same numbers of $\mu^+\mu^-$ and $\tau^+\tau^-$ events were used in [1] for the measurement of forward-backward asymmetry; these are slightly different from those used for the cross-section measurement because of additional requirements to ensure good charge determination.

[2] These are conservative estimates based on comparisons of the results using different programs. The theoretical accuracy of ZFITTER is estimated in [16] to be better than 1% at the LEP 2 energy region.

The contact interaction terms C_2^0 and C_4^0 were evaluated using the improved Born approximation. The value of the effective weak mixing angle $\sin^2\theta_W$ was calculated by ZFITTER. The running QED coupling constant $\alpha(s)$ was used for the s-channel part. The C_2^0, C_4^0 coefficients were then corrected for the effect of photon radiation according to [17]. Initial-state radiation was calculated up to order α^2 in the leading log approximation with soft photon exponentiation, and the order α leading log final state QED correction was applied.

The cross-section for $e^+e^- \to \ell^+\ell^-$ at the centre-of-mass energy point k and $\cos\theta$ bin i is then expressed as a function of $\varepsilon \equiv 1/\Lambda^2$ by

$$\sigma_{i,k}(\varepsilon) = SM_{i,k} + C_2(i,k)\,\varepsilon + C_4(i,k)\,\varepsilon^2 \qquad (e^+e^- \to \ell^+\ell^-)\ , \tag{7}$$

where $SM_{i,k}$ is the Standard Model cross-section. The values of the radiatively corrected contact interaction coefficients, $C_2(i,k)$ and $C_4(i,k)$, were calculated by integrating over each $\cos\theta$ bin i at each centre-of-mass energy point k for each of the contact interaction models and final state fermions considered. Similarly the total cross-section for $e^+e^- \to q\bar{q}$ is defined by

$$\sigma_k(\varepsilon) = SM_k + \sum_{u,d,c,s,b} \left[C_2(k)\,\varepsilon + C_4(k)\,\varepsilon^2\right] \cdot R_{QCD} \qquad (e^+e^- \to q\bar{q})\ , \tag{8}$$

where the additional QCD correction factor $R_{QCD} = 1 + \alpha_s/\pi + 1.409(\alpha_s/\pi)^2$ has been shown separately for the contact interaction terms. The contact interaction is assumed to be independent of the quark flavour.

5 Fit results

The predictions of the contact interaction models were fitted to the data using a binned maximum likelihood method. The likelihood function $\mathcal{L}$ is defined by:

$$\mathcal{L} = \mathcal{G}(r;\Delta r) \prod_{k=1}^{2} \prod_{i=1}^{Nbin} \mathcal{P}(N_{i,k}^{data}, N_{i,k}^{pred}(\varepsilon, r))\ . \tag{9}$$

Here r is a correction to the overall normalisation and $\mathcal{G}(r;\Delta r)$ is the Gaussian probability distribution for r with mean 0 and standard deviation Δr. $\mathcal{P}$ is the Poisson probability of finding $N_{i,k}^{data}$ events of data in the $\cos\theta$ bin i at the centre-of-mass energy point k when $N_{i,k}^{pred}(\varepsilon, r)$ events are predicted. The number of events predicted is given by

$$N_{i,k}^{pred}(\varepsilon, r) = (1 + r)\,[\sigma_{i,k}(\varepsilon) E_{i,k} + B_{i,k}]\,L_k\ , \tag{10}$$

where $\sigma_{i,k}(\varepsilon)$ is the cross-section defined above (equations 7, 8), $E_{i,k}$ is the correction factor for the experimental efficiency, $B_{i,k}$ is the expected background cross-section and L_k is the integrated luminosity. The value of Δr was set to the value of the sum in quadrature of the luminosity error, the systematic error of the event selection and the theoretical uncertainty on the cross-section calculation.

The contact interaction models were fitted to the data with r and $\varepsilon \equiv 1/\Lambda^2$ as fitting parameters. Note that both positive and negative values of ε are physically meaningful. As seen

from equations 2-5, the term $C_2 \cdot \varepsilon$ is linear in η_{ij} and $C_4 \cdot \varepsilon^2$ contains only terms proportional to η_{ij}^2. The results of positive and negative interference with the Standard Model amplitude (sign of η_{ij} parameters) are equivalent under the transformation $\varepsilon \leftrightarrow -\varepsilon$. It is therefore sufficient to fit only for the case of positive interference, but to allow ε to be both positive and negative.

The results of the fits are tabulated in table 3 for the four individual channels. Fits are also made for all the leptonic channels combined ($e^+e^- \to \ell^+\ell^-$) and the lepton and $q\bar{q}$ channels combined (all combined). As described before, for the lepton pair channels the results of the LR and RL models are identical and only the LR results are quoted. The fitted values and their one standard deviation errors on ε are listed in the second column. Figure 1 shows the fitted ε values from the e^+e^-, $\mu^+\mu^-$, $\tau^+\tau^-$, $\ell\ell$ and $\ell\ell + qq$ channels. The error bars in the plots show the positive and negative one standard deviation errors. No significant deviation of the fitted ε from 0 (Standard Model) was observed. The largest deviations are for the $\mu^+\mu^-$ channel by about 2 standard deviations.

Now we check the sensitivity of the present data to the energy scale Λ of the contact interaction. For this purpose the sensitivity estimate λ is defined in terms of the one sided 95 % confidence level upper limit on ε:

$$\lambda = 1/\sqrt{1.64\sigma_\varepsilon} \ ,$$

where σ_ε is the one standard deviation parabolic error on ε. This corresponds to the upper limit on ε allowed for the fluctuation of the data at the 95 % confidence level. The values of λ are listed in the third column of table 3. They are in the range of 1.7 to 5.0 TeV depending on the model and the final state fermion.

The 95 % confidence level lower limit on the energy scale Λ is defined by

$$\Lambda^\pm = 1/\sqrt{\pm\varepsilon^\pm} \ ,$$

where ε^+ and ε^- are the 95 % confidence level limits on ε for positive $(+)$ and negative $(-)$ interference, respectively. The limits $\varepsilon^\pm$ are derived by integrating the probability in the range $\varepsilon > 0$ for the '+' case

$$\int_0^{\varepsilon^+} \mathcal{L}\, d\varepsilon = 0.95 \int_0^\infty \mathcal{L}\, d\varepsilon$$

and $\varepsilon < 0$ for the '$-$' case

$$\int_{\varepsilon^-}^0 \mathcal{L}\, d\varepsilon = 0.95 \int_{-\infty}^0 \mathcal{L}\, d\varepsilon \ .$$

Here $\mathcal{L}$ is the likelihood function given by equation (9). In the integration the overall scale error r was adjusted at each value of ε to maximise the likelihood. It should be noted that the limits on Λ defined in this way tend to be conservative if the true value of ε is close to zero [18]. In previous analyses [3–11, 13] the limits were calculated from the positive and negative one standard deviation errors ($\sigma_\pm$) and the fitted value (ε_0) of ε by $\Lambda^\pm = 1/\sqrt{1.64\sigma_\pm \pm \varepsilon_0}$. However, in that case a problem occurs when ε_0 deviates substantially from 0, where Λ cannot be defined (unphysical region) and the positive and negative limits tend to be quite asymmetric. In order to avoid this problem, λ was used in [10] when $\Lambda > \lambda$.

The results are summarised in the fourth and fifth columns of table 3. The limits on Λ obtained in this way are generally quite close to the sensitivity estimate λ, indicating that

these limits are reasonable. It is seen that the present data are particularly sensitive for the VV and AA models. When all channels are combined the limits on Λ are in the range of 3.4-4.9 TeV for the VV and AA models, and 2.0-3.1 TeV for the other models. Note that, as described in section 2, the coupling constant of the contact interaction is set by convention to $g^2/4\pi = 1$. What is actually constrained by the data is Λ/g. In figure 2 the measured cross-sections are compared with the Standard Model predictions and with contact interaction models VV and AA for $\Lambda^{\pm}$ at the corresponding 95 % confidence level lower limits.

The measured total cross-sections for $e^+e^- \to q\bar{q}$ are lower by up to two standard deviations than the predictions. Note that the contact interaction cannot produce a large negative contribution to the total cross-section for $e^+e^- \to q\bar{q}$ in this energy region and above. This is a consequence of the assumption that the contact interaction is universal for all five quark flavours. The cross-section for an individual quark flavour can deviate either positively or negatively due to interference of the contact interaction with the Standard Model amplitude. The signs of the interferences are opposite for up and down type quarks, and so largely cancel each other. Due to the positive contribution from the $1/\Lambda^4$ term the net result turns out to be insufficient to accommodate the data. Under other assumptions, for example that contact interactions apply only to down (or up) type quarks, both positive and negative deviations may be produced for the $e^+e^- \to q\bar{q}$ cross-section.

6 Conclusion

The differential cross-sections for $e^+e^- \to e^+e^-$, $e^+e^- \to \mu^+\mu^-$, $e^+e^- \to \tau^+\tau^-$ and the total cross-section for $e^+e^- \to q\bar{q}$ at centre-of-mass energies of 130-140 GeV are compared with predictions of the Standard Model and of the contact interaction models. The measured cross-sections are in agreement with the Standard Model expectations. The limits obtained by OPAL on the energy scale Λ are competitive with, or in some cases stronger than, those using existing measurements at lower energies [3–11, 13].

Acknowledgements

We particularly wish to thank the SL Division for the efficient operation of the LEP accelerator and for their continuing close cooperation with our experimental group. In addition to the support staff at our own institutions we are pleased to acknowledge the
Department of Energy, USA,
National Science Foundation, USA,
Particle Physics and Astronomy Research Council, UK,
Natural Sciences and Engineering Research Council, Canada,
Israel Ministry of Science,
Israel Science Foundation, administered by the Israel Academy of Science and Humanities,
Minerva Gesellschaft,
Japanese Ministry of Education, Science and Culture (the Monbusho) and a grant under the Monbusho International Science Research Program,

German Israeli Bi-national Science Foundation (GIF),
Direction des Sciences de la Matière du Commissariat à l'Energie Atomique, France,
Bundesministerium für Bildung, Wissenschaft, Forschung und Technologie, Germany,
National Research Council of Canada,
Hungarian Foundation for Scientific Research, OTKA T-016660, and OTKA F-015089.

References

[1] OPAL Collaboration, G. Alexander et al., Phys. Lett. B376 (1996) 232.

[2] E. Eichten, K. Lane and M. Peskin, Phys. Rev. Lett. 50 (1983) 811.

[3] HRS Collaboration, M. Derrick et al., Phys. Rev. D34 (1986) 3286.

[4] MAC Collaboration, E. Fernandez et al., Phys. Rev. D35 (1987) 10.

[5] CELLO Collaboration, H. J. Behrend et al., Z. Phys. C51 (1991) 149; H. J. Behrend et al., Phys. Lett. B191 (1987) 209; H. J. Behrend et al., Phys. Lett. B222 (1989) 163; H. J. Behrend et al., Z. Phys. C51 (1991) 143.

[6] JADE Collaboration, W. Bartel et al., Z. Phys. C30 (1986) 371.

[7] PLUTO Collaboration, Ch. Berger et al., Z. Phys. C27 (1985) 341.

[8] TASSO Collaboration, W. Braunschweig et al., Z. Phys. C37 (1988) 171; W. Braunschweig et al., Z. Phys. C40 (1988) 163; W. Braunschweig et al., Z. Phys. C43 (1989) 549.

[9] VENUS Collaboration, K. Abe et al., Z. Phys. C48 (1990) 13.

[10] ALEPH Collaboration, Z. Phys C59 (1993) 215.

[11] VENUS Collaboration, K. Abe et al., Phys. Lett. 232B (1989) 425;
TOPAZ Collaboration, I. Adachi et al., Phys. Lett. 255B (1991) 613.

[12] B. Schrempp, F. Schrempp, N. Wermes and D. Zeppenfeld, Nucl. Phys. B296 (1988) 1.

[13] H. Kroha, Phys. Rev. D46 (1992) 58.

[14] W. Beenakker et al., Nucl. Phys. B349 (1991) 323.

[15] D. Bardin et al., CERN-TH 6443/92 (May 1992); Phys. Lett. B255 (1991) 290; Nucl. Phys. B351 (1991) 1; Z. Phys. C44 (1090) 493.

[16] Physics at LEP2, Editors G. Altarelli, T. Sjöstrand and F. Zwirner, CERN 96-01 (February 1996).

[17] Model independent $e^+e^- \to e^+e^-$ lineshape program MIBA,
M. Martinez and R. Miquel, Z. Phys. C53 (1992) 115.

[18] Particle Data Group, L. Montanet et al., 'Statistics' in *Review of Particle Properties*, Phys. Rev. B50 (1994) 1280.

Model	η_{LL}	η_{RR}	η_{LR}	η_{RL}
$LL^{\pm}$	± 1	0	0	0
$RR^{\pm}$	0	± 1	0	0
$VV^{\pm}$	± 1	± 1	± 1	± 1
$AA^{\pm}$	± 1	± 1	∓ 1	∓ 1
$LR^{\pm}$	0	0	± 1	0
$RL^{\pm}$	0	0	0	± 1

Table 1: Different models of the four-fermion contact interaction.

e^+e^-					
		130.26 GeV (2.7 pb^{-1})		136.23 GeV (2.5 pb^{-1})	
$\cos\theta$		N_{ee}	$d\sigma/d\cos\theta$ (pb)	N_{ee}	$d\sigma/d\cos\theta$ (pb)
−0.9 :	−0.7	2	4±3	3	6±4
−0.7 :	−0.5	3	6±3	3	6±4
−0.5 :	−0.3	2	4±3	3	6±4
−0.3 :	−0.1	3	6±3	3	6±4
−0.1 :	0.1	7	13±5	5	10±5
0.1 :	0.3	10	19±6	8	16±6
0.3 :	0.5	27	52±10	12	24±7
0.5 :	0.7	59	113±15	61	123±16
0.7 :	0.9	408	817±41	348	735±39
$\mu^+\mu^-$					
		130.26 GeV (2.7 pb^{-1})		136.23 GeV (2.5 pb^{-1})	
$\cos\theta$		$N_{\mu\mu}$	$d\sigma/d\cos\theta$ (pb)	$N_{\mu\mu}$	$d\sigma/d\cos\theta$ (pb)
−1.0 :	−0.8	0	0	0	0
−0.8 :	−0.6	2	4±3	0	0
−0.6 :	−0.4	1	2±2	0	0
−0.4 :	−0.2	4	7±4	3	6±4
−0.2 :	0.0	0	0	1	2±2
0.0 :	0.2	2	3±3	3	6±3
0.2 :	0.4	5	9±4	2	4±3
0.4 :	0.6	2	3±3	7	14±6
0.6 :	0.8	3	5±4	5	10±5
0.8 :	1.0	6	15±7	7	20±8
$\tau^+\tau^-$					
		130.26 GeV (2.7 pb^{-1})		136.23 GeV (2.5 pb^{-1})	
$\cos\theta$		$N_{\tau\tau}$	$d\sigma/d\cos\theta$ (pb)	$N_{\tau\tau}$	$d\sigma/d\cos\theta$ (pb)
−1.0 :	−0.8	0	0	0	0
−0.8 :	−0.6	0	0	0	0
−0.6 :	−0.4	0	0	0	0
−0.4 :	−0.2	0	0	0	0
−0.2 :	0.0	0	0	0	0
0.0 :	0.2	1	3±3	1	3±3
0.2 :	0.4	2	6±4	2	6±4
0.4 :	0.6	3	9±5	5	16±7
0.6 :	0.8	1	3±3	2	7±5
0.8 :	1.0	2	11±8	0	0

Table 2: Numbers of selected events and differential cross-sections.

Model	ε (TeV^{-2})	λ (TeV)	Λ^- (TeV)	Λ^+ (TeV)
$e^+e^- \to e^+e^-$				
VV	$0.001^{+0.031}_{-0.031}$	4.4	3.6	3.5
AA	$0.057^{+0.051}_{-0.056}$	3.4	2.6	2.7
LL	$0.250^{+0.198}_{-0.175}$	1.8	2.0	1.3
RR	$0.243^{+0.201}_{-0.173}$	1.8	2.0	1.3
LR	$-0.052^{+0.100}_{-0.085}$	2.6	2.2	1.6
$e^+e^- \to \mu^+\mu^-$				
VV	$0.110^{+0.053}_{-0.053}$	3.4	4.1	2.2
AA	$0.160^{+0.070}_{-0.077}$	2.9	3.5	1.9
LL	$0.258^{+0.117}_{-0.119}$	2.3	2.7	1.5
RR	$0.282^{+0.124}_{-0.128}$	2.2	2.5	1.4
LR	$0.200^{+0.156}_{-0.216}$	1.9	1.2	1.5
$e^+e^- \to \tau^+\tau^-$				
VV	$-0.084^{+0.073}_{-0.073}$	2.9	2.2	3.2
AA	$0.010^{+0.077}_{-0.077}$	2.8	2.6	2.5
LL	$-0.114^{+0.174}_{-0.199}$	1.8	1.2	2.0
RR	$-0.132^{+0.200}_{-0.264}$	1.7	1.0	1.9
LR	$-0.147^{+0.184}_{-0.184}$	1.8	1.5	1.9
$e^+e^- \to \ell^+\ell^-$				
VV	$0.020^{+0.026}_{-0.026}$	4.9	4.6	3.7
AA	$0.069^{+0.037}_{-0.038}$	4.0	4.6	2.8
LL	$0.147^{+0.084}_{-0.084}$	2.7	3.0	1.8
RR	$0.160^{+0.090}_{-0.090}$	2.6	2.9	1.8
LR	$-0.055^{+0.092}_{-0.084}$	2.7	2.2	2.2
$e^+e^- \to q\bar{q}$				
VV	$0.025^{+0.072}_{-0.072}$	2.8	3.1	2.7
AA	$-0.067^{+0.079}_{-0.073}$	2.6	2.4	3.4
LL	$-0.134^{+0.158}_{-0.144}$	1.9	1.7	2.4
RR	$0.050^{+0.143}_{-0.145}$	1.9	2.2	1.9
LR	$0.009^{+0.143}_{-0.143}$	2.0	2.0	2.0
RL	$0.178^{+0.149}_{-0.169}$	1.8	2.5	1.6
All combined				
VV	$0.020^{+0.025}_{-0.024}$	5.0	4.9	3.8
AA	$0.038^{+0.029}_{-0.031}$	4.5	4.5	3.4
LL	$0.066^{+0.060}_{-0.065}$	3.1	2.9	2.4
RR	$0.129^{+0.072}_{-0.077}$	2.9	3.1	2.0
LR	$-0.038^{+0.081}_{-0.073}$	2.8	2.4	2.5
RL	$0.009^{+0.080}_{-0.068}$	2.9	2.7	2.2

Table 3: Results of the contact interaction fits.

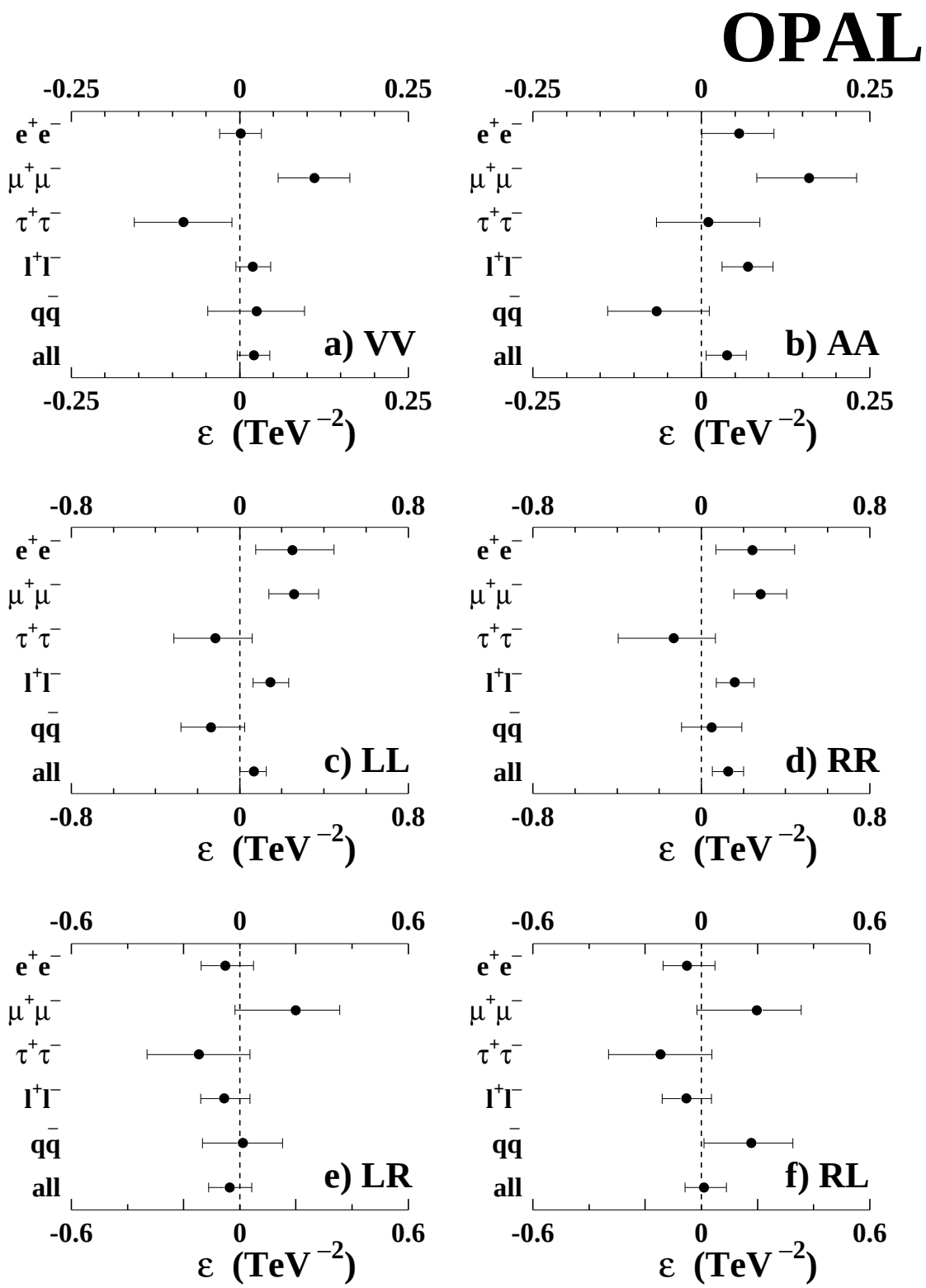

Figure 1: Values of ε (TeV^{-2}) shown with one standard deviation errors for the six contact interaction models. The results for the leptonic channels are identical for the LR and RL.

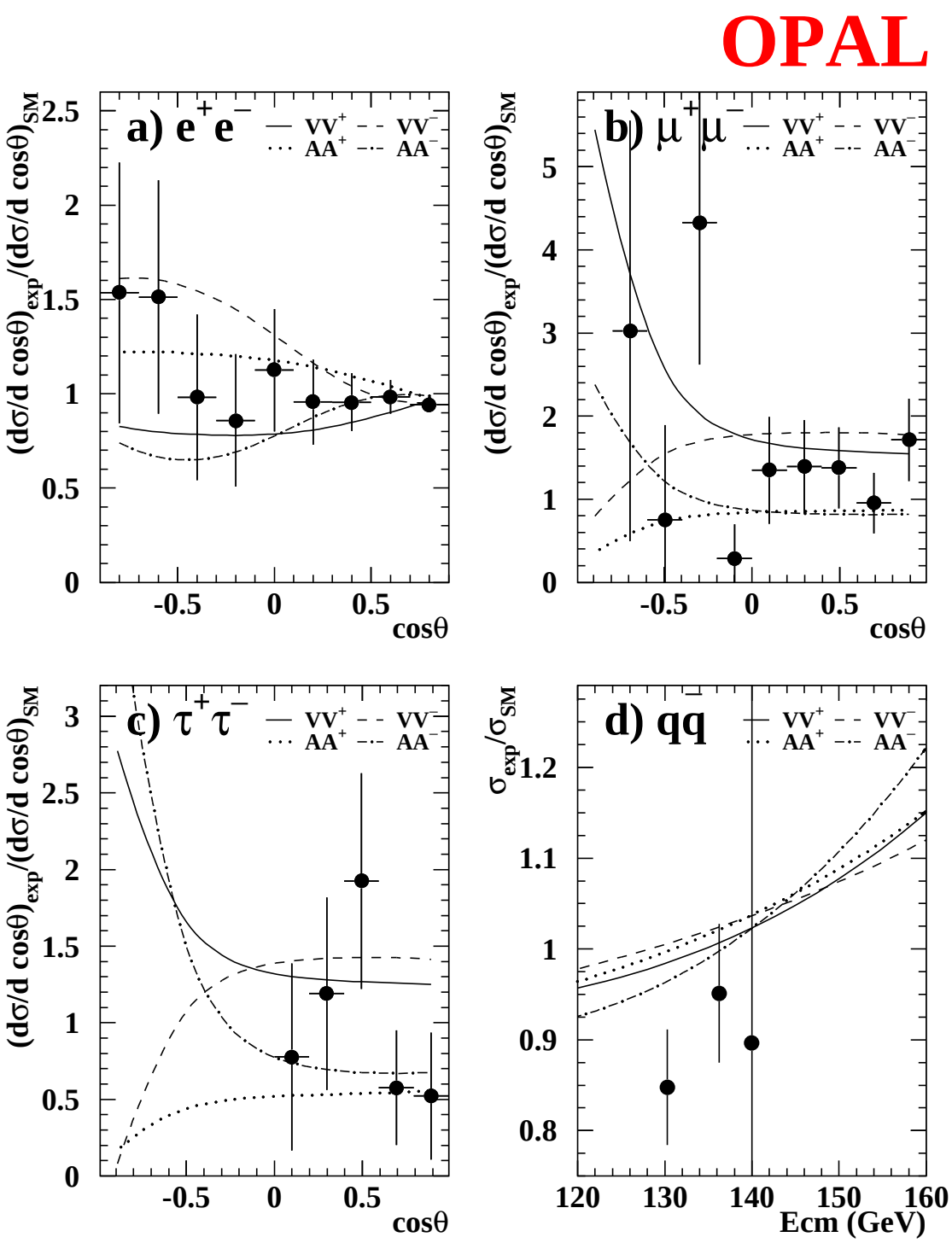

Figure 2: Differential cross-sections normalised to the expectations of the Standard Model for the e^+e^- (a), $\mu^+\mu^-$ (b), $\tau^+\tau^-$ (c) and $q\bar{q}$ (d) channels. The points with error bars are the present measurements and the curves indicate maximum deviations allowed at 95 % confidence level for the VV and AA models.